Control of Chemical Reactions by Convective Turbulence in the Boundary Layer

M. JEROEN MOLEMAKER

Institute for Marine and Atmospheric Research, University of Utrecht, Utrecht, the Netherlands

JORDI VILÀ-GUERAU DE ARELLANO

Departament Fisica Aplicada, Universitat Politècnica de Catalunya, Barcelona, Spain

(Manuscript received 14 February 1996, in final form 4 April 1997)

ABSTRACT

The influence of convective turbulence on chemical reactions in the atmospheric boundary layer is studied by means of direct numerical simulation (DNS). An archetype of turbulent reacting flows is used to study the reaction zones and to obtain a description of the turbulent control of chemical reactions. Several simulations are carried out and classified using a turbulent Damköhler number and a Kolmogorov Damköhler number. Using a classification based on these numbers, it is shown that it is possible to represent and to solve adequately all relevant scales of turbulence and chemistry by means of DNS. The simulations show clearly that the reaction zones are located near the boundaries where the species are introduced. At the lower boundary of the convective boundary layer, the reaction takes place predominantly in the core of the updrafts, whereas in the upper part of the domain the chemical reaction is greatest in the center of the downdrafts. In the bulk of the boundary layer the chemical reaction proceeds very slowly, due to the almost complete segregation of the chemical species. From the point of view of chemistry, the mixing across the interface between updrafts and downdrafts in the bulk of the convective boundary layer plays only a minor role.

The amount of chemical reaction in relation to the degree of turbulence is quantified by the introduction of an effective Damköhler number. This dimensionless number explicitly takes into account the reduction of the reaction rate due to the segregation of the chemical species. It is shown that the number approaches an asymptotic value that is $O(1)$ for increasingly fast reaction rates. This shows explicitly that the timescale of the chemical reactions is limited by the integral turbulent timescale. It is suggested how a parameterization could be used to include this effect into one-dimensional atmospheric models.

1. Introduction

The convective boundary layer (CBL) in the atmosphere is a chemical environment in which the chemical species are not well mixed. This is unlike a chemical reaction chamber in which all species are homogeneously mixed. The turbulent structure of the CBL can be characterized by narrow and vigorous upward motions combined with wide and slow downward motions (Lenschow and Stephans 1980; Moeng and Wyngaard 1984). Compounds emitted at the surface or entrained at the top of the CBL are transported by these updrafts and downdrafts. With regard to passive scalars, several studies (Wyngaard and Brost 1984; Chatfield and Brost 1987; Piper et al. 1995) have shown the importance of taking the turbulent characteristics of the CBL into account, particularly the differences between transport of scalars by the updrafts and by the downdrafts.

Corresponding author address: Dr. M. Jeroen Molemaker, Institute for Marine and Atmospheric Research, University of Utrecht, Princetonplein 5, 3584 CC Utrecht, the Netherlands.
E-mail: nmolem@fys.ruu.nl

An archetypical case has been widely studied. This case is the top-down (bottom-up) diffusion of a scalar: a scalar is emitted at the upper (lower) boundary and its flux at the opposite boundary is assumed to be zero. The emitted compound at the lower boundary is transported initially by updrafts and the compound emitted at the upper boundary initially by downdrafts. As a consequence, both compounds are segregated and the covariance between the concentrations of the two compounds will be negative. Aircraft measurements of temperature and moisture (considering these two variables as scalars), as analyzed by Wyngaard et al. (1978), confirmed this behavior.

The inhomogeneity of the CBL and therefore the segregation of the chemical compounds play a key role if the compounds react with a second- or higher-order chemical reaction. A similar feature can be found in other studies of turbulent reacting flows (Libby and Williams 1980; Galperin and Orszag 1993). It is essential to represent the actual chemical reaction rate correctly in order to obtain accurate values of the concentration of the product species. These product species initiate a chemical reaction chain composed either of first-order

chemical reactions (which are triggered by UV radiation, and therefore their highest chemical reaction rates occur under convective conditions) or of second-order chemical reactions (Seinfeld 1986). Segregation of species is represented in the ensemble average of the conservation equation of chemical species by the concentration covariance term (Donaldson and Hilst 1972). When the timescale of turbulence is comparable to the timescale of chemistry—that is, a moderate chemistry regime—the covariance is of the same order of magnitude as the product of the ensemble averaged concentrations. In the atmospheric CBL, species that react in this regime are the nitrogen oxides and ozone (Dennis et al. 1996). The case of bottom-up and top-down diffusion of two chemically reactive species has been studied previously by Schumann (1989) and Sykes et al. (1994) using the large eddy simulation (LES) technique. All these studies included a detailed analysis of this turbulent reacting flow in the CBL. Schumann (1989) described the main features of the flow and calculated profiles of the concentration covariance. He introduced the two dimensionless numbers that characterized the flow: a turbulent Damköhler number (the ratio of the integral turbulent timescale to the chemical reaction timescale) and the ratio of the entrainment flux to the emission flux of the two chemical species. In our study, an extra dimensionless number, the Kolmogorov Damköhler number, has been added to the numbers mentioned above to classify the turbulent reacting flows. This number is the ratio of the Kolmogorov timescale to the chemical timescale (Bilger 1980). Hence, the mixing of the largest scales that are present in the flow is represented by the turbulent Damköhler number and the Kolmogorov Damköhler number characterizes the smallest mixing scales. A classification of turbulent reacting flows is given as a function of the two Damköhler numbers.

Sykes et al. (1994) used results of an LES to propose several third-order closure models that are necessary to close the second-order equations for the covariance between two chemically reactive species. B96 presented the budget analysis of the concentration fluxes and the concentration covariances of the chemical species. Analyzing the second-order moments of these variables, they conclude that the chemical terms of these equations cannot be neglected.

All of the above-mentioned studies state that the amount of turbulence available determines the chemical reaction rates. In other words, the chemical reaction rate depends on the ability of the turbulent flow to bring the two chemical species together. However, to our knowledge, this turbulence control has never been studied quantitatively as a function of the Damköhler numbers. In the work to follow, we will quantify this control of the turbulence by defining and calculating a chemical reaction rate that includes the effect of turbulence. Moreover, we will give special attention to the location of the reaction zones and to the amount of reaction that takes place in the updrafts and in the downdrafts, using conditional averaging.

We will consider an idealized turbulent reacting flow in a buoyancy-driven boundary layer. This flow has been simulated using a direct numerical simulation (DNS). Our study was inspired by the work of (Moeng and Rotunno 1990) where a similar tool was used to explain the disagreement between vertical velocity skewness observations and LES results. In Herring and Wyngaard (1987), a DNS was also used to study chemical species that react with a first-order chemical reaction in the CBL.

The advantage of a DNS over an LES is that all the scales of the flow are solved explicitly and consequently no assumptions have to be made about the subgrid contributions of the chemical reactions (Colenman et al. 1990). The fact that all scales have to be resolved explicitly means of course that the Reynolds number Re of the simulated flow is restricted to relatively low values. However, in the Reynolds number similarity regime the properties of turbulent flows are independent of the Reynolds number (Tennekes and Lumley 1973). We believe that our simulated flow is in this asymptotic regime and hence the results obtained here can be applied to the CBL in a straightforward way (Moeng and Rotunno 1990).

In this paper, the flux at the lower boundary of one of the species is equal to the flux at the upper boundary of the other species. As a result, after a certain time, a balance will be achieved between the input of chemical species and chemical reaction. At this time the volume-averaged concentrations of the two chemical species reach a quasi-steady state. An effective turbulent Damköhler number based on the volume-averaged concentrations and their intensity of segregation in the steady state will be defined. This effective Damköhler number explicitly takes into account the effect of turbulence on the chemical reaction.

The numerical model used is described in section 2. In section 3 the main characteristics of the flow are described. An analysis of the reaction zones, classified according to the two Damköhler numbers, is presented in section 4. In section 5, the turbulent control of chemical reactions in the CBL is studied and a parameterization that takes this control into account is proposed. Section 6 summarizes the most important conclusions.

2. Problem formulation

Consider a three-dimensional incompressible fluid, with constant kinematic viscosity ν and diffusivity of heat κ in a rectangular box of aspect ratio A_x, A_y (ratio of the two horizontal extensions L and W to height H). At the bottom of the fluid a constant heat flux F_0 is prescribed, which heats the layer from below.

The governing equations are made nondimensional by using the following scales: H, H^2/κ, κ/H, and HF_0/κ

for length, time, velocity, and temperature, respectively. If the velocity is $\mathbf{u} = (u, v, w)$ and the (potential) temperature is T, assuming the Boussinesq approximation and a linear equation of state, the dimensionless governing equations read

$$\mathrm{Pr}^{-1}\left(\frac{\partial \mathbf{u}}{\partial t} + \mathbf{u}\cdot\boldsymbol{\nabla}\mathbf{u}\right) = -\boldsymbol{\nabla}p + \nabla^2\mathbf{u} + \mathbf{e}_3\mathrm{Ra}_\mathrm{f}T \quad (1a)$$

$$\boldsymbol{\nabla}\cdot\mathbf{u} = 0 \quad (1b)$$

$$\frac{\partial T}{\partial t} + \mathbf{u}\cdot\boldsymbol{\nabla}T = \nabla^2 T, \quad (1c)$$

where Pr is the Prandtl number, Ra_f the flux Rayleigh number, and $\mathbf{e}_3$ the unit vector in the vertical direction. Two chemically reactive species A, B are introduced into this fluid, each with the same molecular diffusivity κ_C. Species A is emitted from the bottom boundary with a constant flux F_A and a flux F_B is specified at the top for species B. Here, F_A will be positive and F_B will be negative representing an input of each species at the respective boundaries.

The species react with a second-order isothermal irreversible binary reaction at a reaction coefficient rate k. The conservation equations for the two species are made nondimensional using the above-mentioned scales and the two concentration scales are defined as HF_A/κ_C and HF_B/κ_C. The equations then read

$$\frac{\partial C_A}{\partial t} + \mathbf{u}\cdot\boldsymbol{\nabla}C_A = -n\mathrm{Da}_\mathrm{d}C_AC_B + \mathrm{Le}^{-1}\nabla^2 C_A \quad (2a)$$

$$\frac{\partial C_B}{\partial t} + \mathbf{u}\cdot\boldsymbol{\nabla}C_B = -\mathrm{Da}_\mathrm{d}C_AC_B + \mathrm{Le}^{-1}\nabla^2 C_B, \quad (2b)$$

where C_A, C_B are the dimensionless concentrations of species A, B. Here Da_d is a diffusive Damköhler number, n is the flux ratio (F_B/F_A), and Le is the Lewis number for both species. These dimensionless numbers are defined as

$$\mathrm{Ra}_\mathrm{f} = \frac{g\alpha H^4 F_0}{\nu\kappa^2}, \qquad \mathrm{Pr} = \frac{\nu}{\kappa}, \qquad \mathrm{Da}_\mathrm{d} = \frac{kH^3F_A}{\kappa\kappa_C},$$

$$\mathrm{Le} = \frac{\kappa}{\kappa_C}, \quad (3)$$

where α is the expansion coefficient for temperature.

Periodic boundary conditions are prescribed in the horizontal. At the upper and lower boundaries stress-free conditions are prescribed for the velocity field. The dimensionless boundary conditions for the temperature and the chemical species at the upper and lower boundaries are

$$z = 0: \qquad \frac{\partial T}{\partial z} = 1, \qquad \frac{\partial C_A}{\partial z} = 1, \qquad \frac{\partial C_B}{\partial z} = 0 \quad (4a)$$

$$z = 1: \qquad \frac{\partial T}{\partial z} = 0, \qquad \frac{\partial C_A}{\partial z} = 0, \qquad \frac{\partial C_B}{\partial z} = -1. \quad (4b)$$

Using these boundary conditions we simulate the case of the bottom-up diffusion of species C_A and the top-down diffusion of species C_B.

Numerical methods

Equations (1) and (2) are discretized on an equidistant staggered grid. The discretized momentum equations together with the boundary conditions constitute a set of (coupled) ordinary differential equations of the form

$$\frac{d\mathbf{u}_{i,j,k}}{dt} = -\boldsymbol{\nabla}p_{i,j,k} + \mathbf{F}_{i,j,k}(\mathbf{u}, T) \quad (5)$$

for $i = 1, \ldots, N$, $j = 1, \ldots, M$, and $k = 1, \ldots, L$. In Eq. (9), $\mathbf{F}_{i,j,k}$ contains the (discretized) advective, diffusive, and buoyancy terms from Eq. (1b). This set of equations is integrated in time using an Adams–Bashforth method (second-order accurate in time), which reads

$$\mathbf{u}^{n+1}_{i,j,k} = \mathbf{u}^n_{i,j,k} + \Delta t\left(\frac{3}{2}(\mathbf{F}^n_{i,j,k} - \boldsymbol{\nabla}p^n_{i,j,k}) - \frac{1}{2}(\mathbf{F}^{n-1}_{i,j,k} - \boldsymbol{\nabla}p^{n-1}_{i,j,k})\right). \quad (6)$$

Taking the divergence of (6) yields

$$D^{n+1}_{i,j,k} = D^n_{i,j,k} + \Delta t\left(\frac{3}{2}(R^n_{i,j,k} - \nabla^2 p^n_{i,j,k}) - \frac{1}{2}(R^{n-1}_{i,j,k} - \nabla^2 p^{n-1}_{i,j,k})\right), \quad (7)$$

where $D = \boldsymbol{\nabla}\cdot\mathbf{u}$ and $R = \boldsymbol{\nabla}\cdot\mathbf{F}$. In this case the pressure term acts as a constraint that ensures that the flow will remain divergence free. To calculate the pressure at every time step, we rearrange (7) and demand that

$$D^{n+1}_{i,j,k} = 0$$

$$\nabla^2 p^n_{i,j,k} = \frac{2}{3}D^n_{i,j,k} + \Delta t\left(R^n_{i,j,k} - \frac{1}{3}(R^{n-1}_{i,j,k} - \nabla^2 p^{n-1}_{i,j,k})\right). \quad (8)$$

At time n all the terms on the right-hand side of (8) are known, so we can solve for $p^n_{i,j,k}$. In the horizontal directions, periodicity is assumed. Boundary conditions at $z = 0$, 1 for (8) are found using (1b) and using the fact that at the upper and lower boundary $w = 0$. As a consequence, these boundary conditions for (8) can be written thus:

$$z = 0, 1: \qquad \frac{\partial p}{\partial z} = \frac{\partial^2 w}{\partial z^2} + \mathrm{Ra}_\mathrm{f}T. \quad (9)$$

Due to the central differences schemes, small negative concentrations may develop because of numerical errors especially when there are steep gradients in the concentration. Following Riley et al. (1986), negative values of reactant concentrations were set to zero at regular

intervals during the simulations. As a check for sufficient accuracy, the volume-integrated budgets for the chemical species were calculated. These budgets were found to be correct within 0.1% during all simulations.

3. Flow characteristics

In all the simulations, the following nondimensional numbers characterize the flow: $\mathrm{Ra_f} = 10^7$, $\mathrm{Pr} = 1$, and $\mathrm{Le} = 1$. The domain was defined by the aspect ratio $A_x = A_y = 4$. As a measure of the smallest relevant scales in the flow, the Kolmogorov length scale $\eta^* = (\nu^3/\epsilon^*)^{1/4}$ (from now on * denotes a dimensional dependent quantity) is used (Tennekes and Lumley 1973) where ϵ^* is the dissipation of turbulent kinetic energy. The dissipation is assumed to be constant over the domain and can be estimated by assuming that the dissipation term is equal to the production term that represents the buoyancy forces in the turbulent kinetic energy equation. Therefore,

$$\epsilon^* = g\alpha w^* T^*. \tag{10}$$

Using the Kolmogorov length scale and expression (10), one can establish a relation between the intensity of the turbulent flow (characterized by the flux Rayleigh number) and the smallest scale of the flow that contains energy. Using the nondimensional scales defined in section 2 and approximating w^*T^* by the heat flux F_0, the following relation is found:

$$\eta = (1/\mathrm{Ra_f})^{1/4}, \tag{11}$$

where η is now a dimensionless Kolmogorov length. Following Grotzbach (1983), we may use η as an estimate of the minimum grid width Δ necessary to resolve all relevant scales of the simulated variables. This condition is expressed as

$$\Delta \leq \pi\eta. \tag{12}$$

The numerical resolution used was $(64 \times 64 \times 64)$ grid points, which is just sufficient to resolve all horizontal scales. We performed one test run at a higher horizontal resolution $(128 \times 128 \times 64)$ and found that all large-scale features of the flow were solved to within 1% accuracy using a 64^3 grid. The time step used for time integration was 10^{-5}.

In all the simulations, the parameters that characterize the flow are kept invariant and only the chemical reaction rate is varied—that is, the diffusive Damköhler number is changed. The convective velocity scale for the simulations is determined by the driving heat flux and it is defined as $w_c^* = (Hg\alpha F_0)^{1/3}$ (Deardorff 1972). The dimensionless convective velocity $w_c = (\mathrm{Ra_f Pr})^{1/3}$, for $\mathrm{Ra_f} = 10^7$ (all simulations) is equal to 215. This setting of the parameters may be applied to many corresponding dimensional situations. Table 1 lists dimensional quantities that correspond to this parameter setting if we apply the result to a typical atmospheric convective boundary layer. Note that since the reaction rate k and the flux of the chemical species F_A appear together as a product in the definition of the control parameter $\mathrm{Da_d}$ varying the fluxes of the chemical species is equivalent to varying the reaction rate.

TABLE 1. Corresponding dimensional quantities for an application to an atmospheric convective boundary layer. Here K_H and K_M are (constant) subgrid diffusivities for heat and momentum, respectively. The value of F_0 corresponds with a heat flux of 120 W m^{-2}.

H	10^3 m
K_H	7 m^2 s^{-1}
K_M	7 m^2 s^{-1}
F_0	0.1 K m s^{-1}
w_c^*	1.5 m s^{-1}
k	10^{-4} ppb^{-1} s^{-1}
F_A	0.1 − 10 ppb m s^{-1}
F_B	0.1 − 10 ppb m s^{-1}

All nondimensional velocity statistics presented will be scaled using w_c^*. Figure 1 shows the vertical profile of the velocity variances and the flux of vertical velocity. These variables are horizontally averaged over the domain (denoted by an overbar). The results obtained compare well with results obtained previously using large eddy simulations (Moeng 1984), direct numerical simulations (Moeng and Rotunno 1990), and laboratory experiments (Deardorff and Willis 1967). The main difference is that the horizontal velocity variances are not zero at the horizontal boundaries, due to the different (stress-free) boundary conditions prescribed in the simulations used here. We believe that this difference in boundary conditions will have only a minor quantitative effect on volume-averaged properties in convectively driven flows, which will be even smaller for flows with a higher Rayleigh number since the flow is affected only by the different boundary conditions in the thin boundary layers near the walls that will become even narrower if the Rayleigh number is increased.

Figure 2 shows spectra of the horizontal and vertical velocity components v and w and the chemical reaction term. The velocity spectra are normalized using the velocity scale w_c^* and the spectrum of the reaction product is normalized using the concentration scale $\langle C_A \rangle$ where $\langle\ \rangle$ denotes a volume average. All normalized spectra are now $O(1)$. All spectra were obtained by averaging 1D spectra in the x direction over the whole domain. The resulting spectra were also averaged in time over a convective timescale. Figure 2a shows that all velocity scales are resolved to within the dissipative range. An inertial subrange dividing production scales and dissipating scales is not clearly established, which is in accordance with previous studies (Grotzbach 1982; Herring and Wyngaard 1987). Figure 2b shows that the spectrum of the covariance between the two species decays according to $k^{-2/3}$. The test run (not plotted) at a higher resolution shows that this power spectrum should fall off slightly faster (like the power spectra of the velocities components) and that the resolution used is only just sufficient. However, the larger scales and

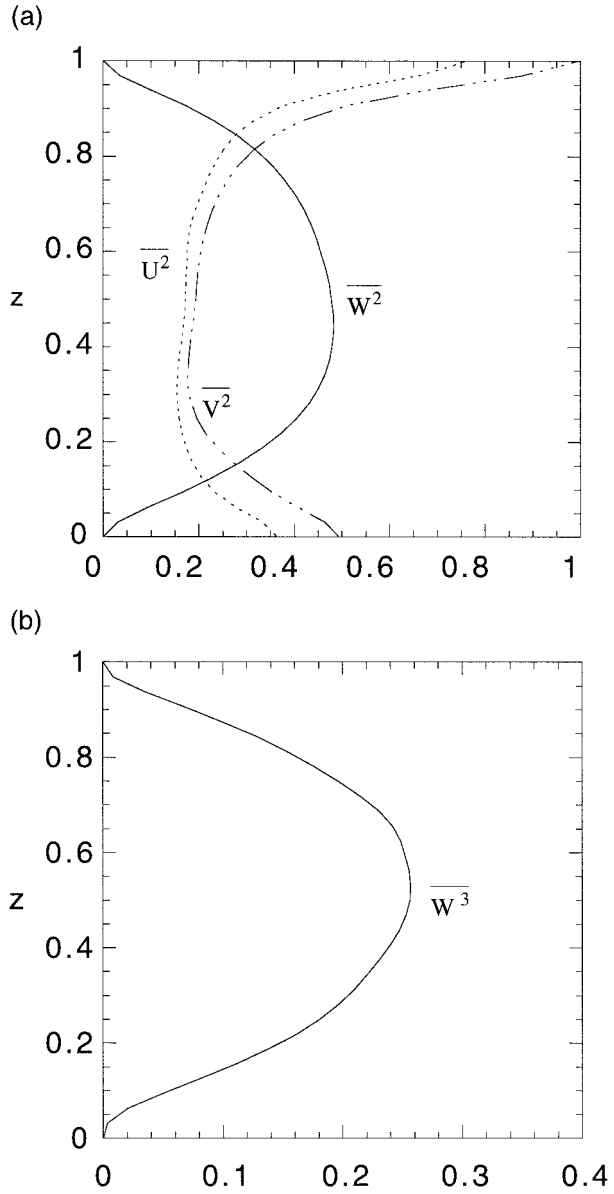

FIG. 1. Vertical profiles of (a) the dimensionless velocity variances and (b) the dimensionless flux of vertical-velocity variance.

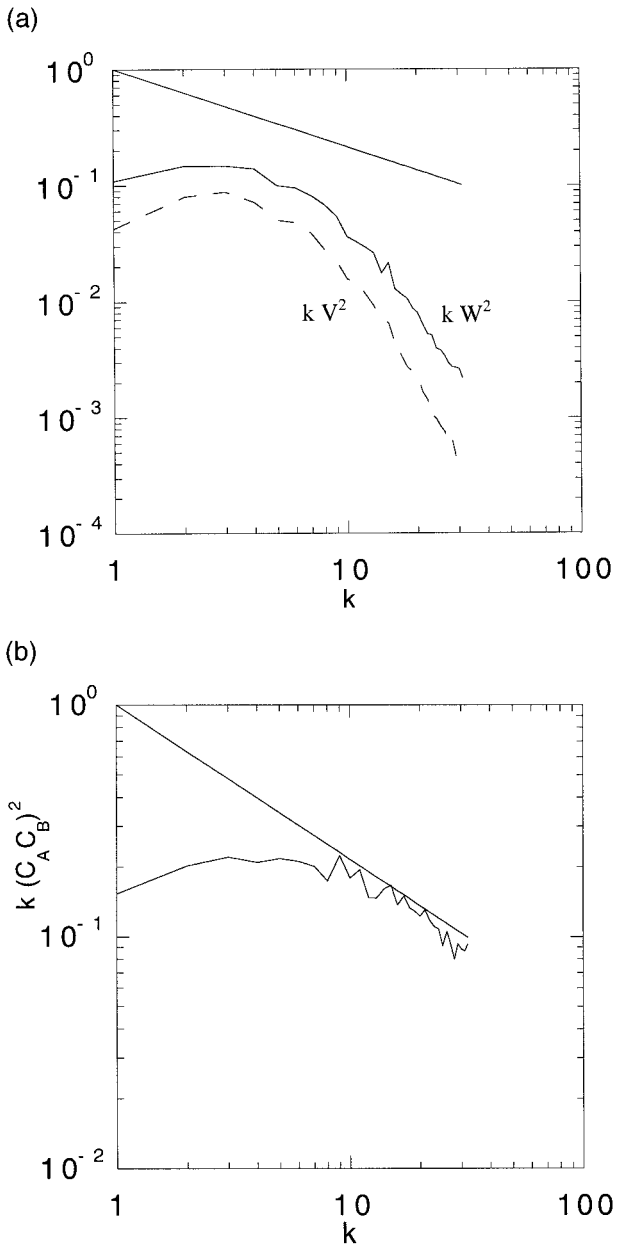

FIG. 2. (a) One-dimensional power spectra of horizontal (v) and vertical velocity fluctuations (w) and (b) 1D spectrum of covariance between both chemical species (simulation 4). Spectra have been averaged in space and time.

the horizontally averaged or volume-averaged quantities related to the chemical species did not change significantly.

If the flow is within the turbulent regime (as is the flow considered here), the characteristics of the flow become independent of the Reynolds number of the flow. Therefore, we may apply the results of the simulations presented in this paper to flows with a much higher Reynolds number, such as the atmospheric CBL. This is also confirmed by a direct comparison between some of the results presented here and an LES of the CBL (Betts et al. 1996). If we use the simulations presented to represent the CBL this is equivalent to using an LES with a very simple subgrid model; that is, constant eddy diffusivity coefficients. We have chosen to use a numerical model without intricate subgrid-scale parameterization in order not to cloud any of the physics present in the interaction between turbulence and chemistry.

4. Reaction zones

As stated before, chemical species are not perfectly mixed in the CBL. It is therefore important to determine

in which zones of the convective boundary layer the reaction takes place. To classify the various numerical simulations, two dimensionless numbers are introduced. One is the turbulent Damköhler number $\mathrm{Da_t}$, which is the ratio of the integral turbulent timescale to the chemical reaction timescale and is defined as

$$\mathrm{Da_t} = \frac{H}{w_c^*} k\langle C^* \rangle, \tag{13}$$

where $\langle C^* \rangle$ is the (dimensional) volume-averaged concentration of one of the species in steady state. This number accounts for the mixing yield produced by the large eddies. The chemical reaction timescale is estimated here using the volume-averaged concentration of the species. This definition differs from the one proposed by Schumann (1989), where the concentration is scaled using the emission flux. The definition proposed here is based on the actual concentration and consequently it is a better representation of the true chemical reaction timescale. The other number is the Kolmogorov Damköhler number $\mathrm{Da_k}$, which is the ratio of the Kolmogorov timescale to the chemical reaction timescale and is defined as

$$\mathrm{Da_k} = \left(\frac{\nu}{\epsilon^*}\right)^{(1/2)} k\langle C^* \rangle. \tag{14}$$

This dimensionless number relates the mixing activity of the smallest energy containing turbulent scales to the chemical reaction rate. Using these two Damköhler numbers, a complete classification of turbulent reacting flows can be established that embraces all the relevant scales. On the basis of these two numbers, Bilger (1980) introduced the following classification of turbulent reacting flows:

$\mathrm{Da_t} \ll 1$ slow chemistry,

$\mathrm{Da_k} < 1 < \mathrm{Da_t}$ moderate chemistry,

$\mathrm{Da_k} \gg 1$ fast chemistry.

Slow chemistry implies that the chemistry is slower than the integral timescale of turbulence. Moderate chemistry means here that the chemistry timescale is shorter than the integral timescale but longer than the Kolmogorov timescale of the flow. Fast chemistry finally signifies a chemical timescale that is shorter than the Kolmogorov timescale—that is, combustion processes. To our knowledge this classification has not been applied to turbulent reacting flows under convective conditions.

The ratio of the flux at the lower boundary of species A to the flux of species B at the upper boundary (n) is set to -1 for all the simulations; this ratio corresponds to equal but opposite fluxes of the two chemical species. The initial concentrations of the two chemical species are set to zero and consequently the species are not premixed. If the fluxes are equal, the volume-averaged concentrations of the chemical species will reach a quasi-steady state after a few turbulent timescales. Moreover, if the prescribed fluxes and the initial concentrations of the species are equal, it is evident that the volume-averaged concentrations of both species $\langle C_A \rangle$ and $\langle C_B \rangle$ will be equal at all times. Therefore, only one turbulent Damköhler number and one Kolmogorov Damköhler number are necessary to characterize the various simulations. Table 2 summarizes the results obtained in the numerical simulations where only $\mathrm{Da_d}$ is varied and all other parameters specified in (3) are kept constant (I_s and $\mathrm{Da_e}$ will be defined later). As can be seen from the table, the simulations ranged from the slow chemistry regime to the moderate chemistry regime. For all the simulations $\mathrm{Da_k} < 1$ and if Le = 1, as in the present case, the length scales associated with the chemical reaction are always larger than the Kolmogorov length scales and are therefore explicitly calculated in the simulations. The range of the numerical experiments was selected in order to analyze the effect of the intensity of turbulence on the amount of chemical reaction as a function of $\mathrm{Da_t}$. The range of $\mathrm{Da_t}$ and $\mathrm{Da_k}$ is representative for certain chemical reactions in the atmospheric convective boundary layer (Seinfeld 1986; Stockwell 1995; Dennis et al. 1996).

TABLE 2. Summary of the numerical simulations. The only varying control parameter is $\mathrm{Da_d}$; all other quantities are derived from the quasi-steady state that is reached after a few convective timescales.

Simulation	$\mathrm{Da_d}$	$\langle C \rangle$	$\mathrm{Da_t}$	$\mathrm{Da_k}$	$\langle I_s \rangle$	$\mathrm{Da_e}$
1	$4.6\ 10^3$	0.016	0.34	0.023	−0.15	0.29
2	$9.2\ 10^3$	0.012	0.53	0.036	−0.30	0.37
3	$2.3\ 10^4$	0.010	1.07	0.073	−0.57	0.46
4	$4.6\ 10^4$	0.008	1.71	0.117	−0.66	0.58
5	$1.2\ 10^5$	0.006	3.80	0.259	−0.83	0.65
6	$2.8\ 10^5$	0.006	8.09	0.552	−0.91	0.73
7	$4.6\ 10^5$	0.006	13.27	0.904	−0.94	0.75

Figure 3a shows the concentration profiles of both species for $\mathrm{Da_d} = 4.6 \times 10^4$. These profiles are typical for all the numerical experiments. Although the transport of both species is asymmetric, the resulting mean concentration profiles are only slightly asymmetric. This is in agreement with the horizontally averaged concentration profiles for passive tracers presented by Wyngaard and Brost (1984) and for chemically reactive species found by Schumann (1989). As can be seen from the figure, sharp concentration gradients are present at the bottom and top of the boundary layer where the two species are introduced. The flux profiles of the bottom-up species and top-down species are shown in Fig. 3b. In the absence of chemical reactions, the flux profile is linear. The flux profiles of the chemical species become strongly nonlinear when chemical reactions are present. From the figure it is clear that the nonlinearity of the flux profiles is most pronounced near the lower and upper boundaries where most of the chemical reaction takes place.

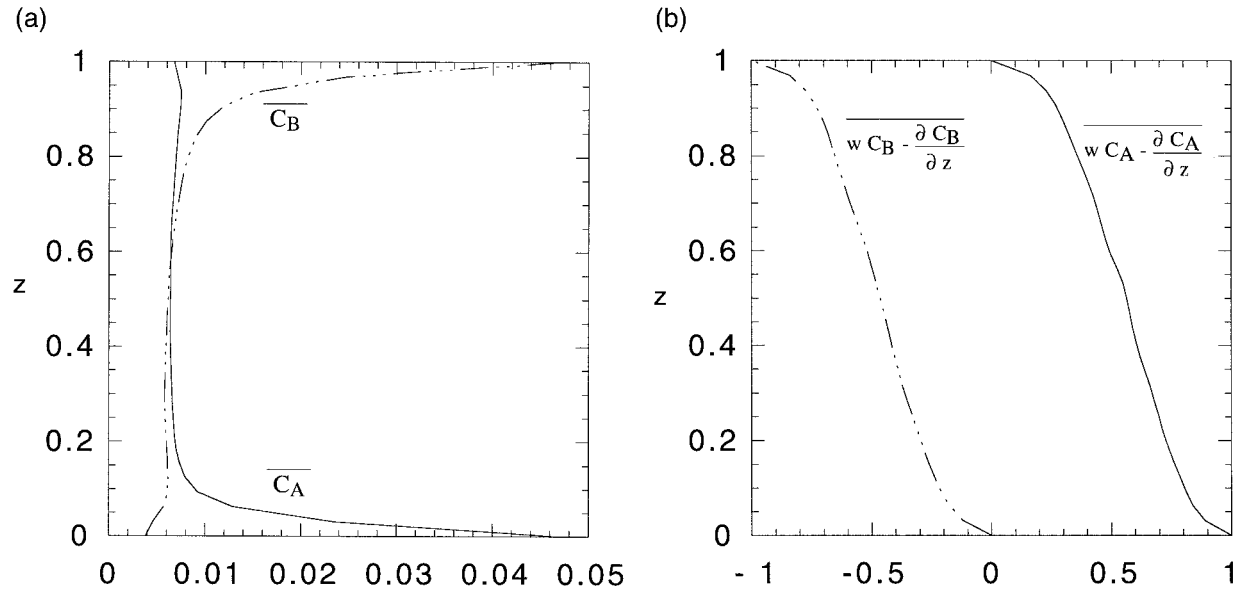

FIG. 3. Vertical profiles ($Da_d = 4.6 \times 10^4$) of (a) the dimensionless horizontally averaged concentration of chemical species and (b) the dimensionless total vertical flux of the chemical species.

These flux profiles are similar to those calculated by Gao and Wesley (1994) using a one-dimensional model for a neutral atmospheric boundary layer that included chemistry.

To show in which part of the boundary layer the chemical reaction takes place, three horizontal cross sections of the reaction product kC_AC_B are depicted in Fig. 4 for the simulation in which $Da_d = 4.6 \times 10^4$. In all cross sections the values are scaled with their absolute maximum value. In Fig. 4a it is shown that at $z = 0.1$, near the lower boundary, the reaction takes place in the core of the updraft, whereas near the top at $z = 0.9$ (Fig. 4c), the reaction occurs in the downdraft. Note that the maximum value of the reaction product for $z = 0.5$ is about one order of magnitude smaller than the maximum values for $z = 0.1$ and $z = 0.9$. So, in the bulk of the boundary layer, the reaction rate is close to zero, due to the almost complete segregation of chemical species. Consequently, the role of the mixing across the interface between the updrafts and downdrafts is not important. Therefore, from the point of view of chemistry, lateral horizontal mixing is important near the lower and upper boundaries, in those regions where the chemical species are introduced, and plays only a minor role in the bulk of the boundary layer.

For larger Damköhler numbers, the same features have been observed, but the reaction zones are horizontally narrower and closer to the lower and upper boundaries. This physical description shows that the separated transport of species *A* and *B* (Wyngaard and Weil 1991; Schumann 1993) strongly influences the performance of chemical reactions. An analysis of the second-order moment equations for chemical species clearly shows the necessity of introducing the chemical terms into these equations and the dependence of these terms on the Damköhler numbers and the flux ratio (Vilà-Guerau de Arellano et al. 1995).

In order to quantify how the chemical reaction is distributed over updrafts and downdrafts, the vertical profile of the area fraction of the reaction product is shown in Fig. 5. These area fractions are defined as

$$A_{\text{up}} = \frac{[C_AC_B]_{\text{up}}}{[C_AC_B]_{\text{up}} + [C_AC_B]_{\text{down}}} \tag{15a}$$

$$A_{\text{down}} = \frac{[C_AC_B]_{\text{down}}}{[C_AC_B]_{\text{up}} + [C_AC_B]_{\text{down}}}, \tag{15b}$$

where the square brackets signify a horizontal integral, either over the updrafts (defined by a positive vertical velocity) or over the downdrafts. For all the cases analyzed, around 70% of the chemical reaction occurs in the updrafts in the lower 10% of the domain. This behavior is reversed in the upper boundary; there most of the chemical reaction takes place in the downdrafts (around 80%).

5. Chemical reaction rate limited by turbulence

The amount of chemical reaction is determined by the ability of turbulence to bring the species together (Donaldson and Hilst 1972). In any situation where the chemical components are not premixed but introduced at opposite boundaries, as studied here, the reaction rate will be slower than when both species are perfectly mixed. This can be seen clearly from the horizontally

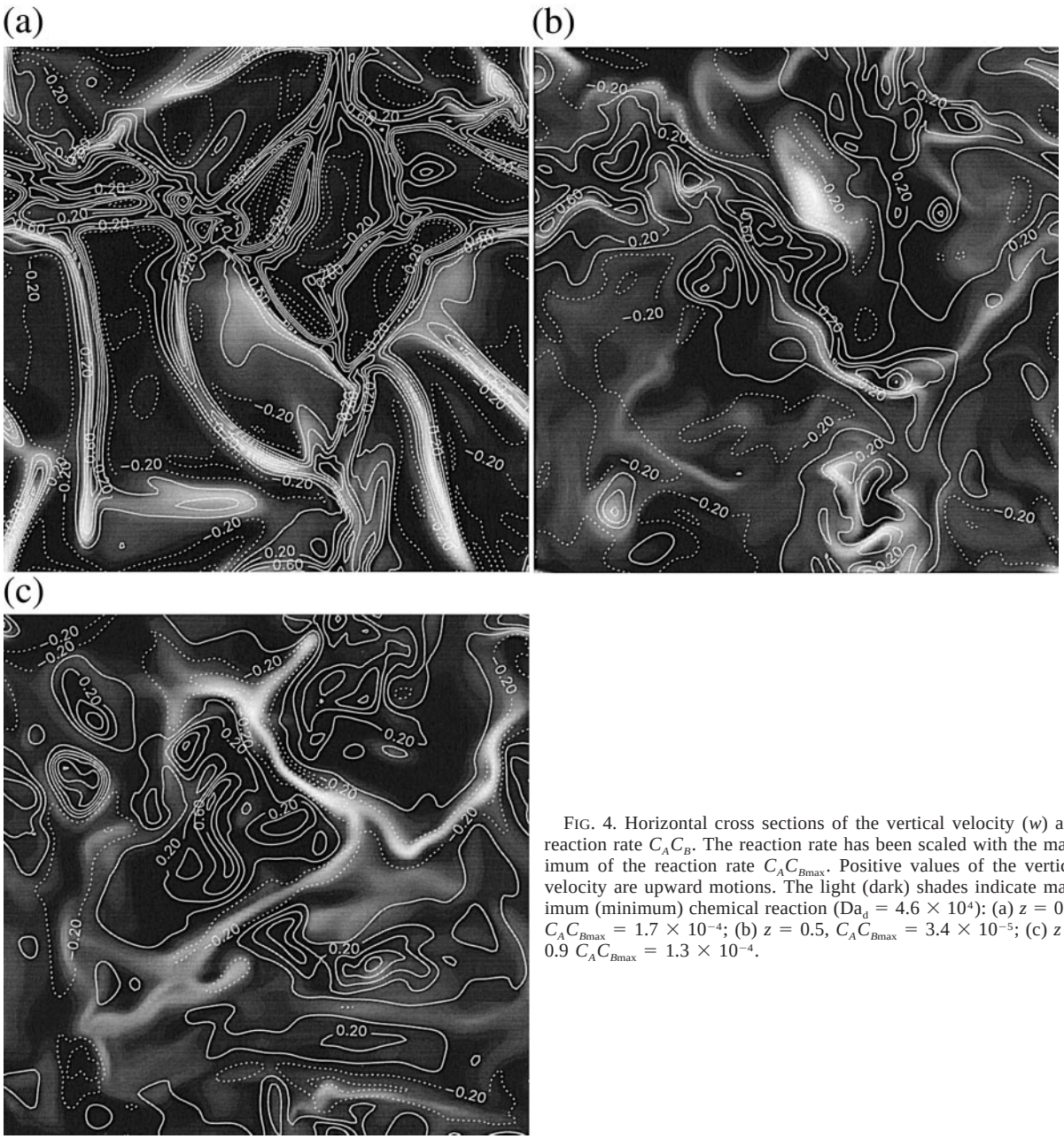

FIG. 4. Horizontal cross sections of the vertical velocity (w) and reaction rate $C_A C_B$. The reaction rate has been scaled with the maximum of the reaction rate $C_A C_{B\max}$. Positive values of the vertical velocity are upward motions. The light (dark) shades indicate maximum (minimum) chemical reaction ($\mathrm{Da_d} = 4.6 \times 10^4$): (a) $z = 0.1$, $C_A C_{B\max} = 1.7 \times 10^{-4}$; (b) $z = 0.5$, $C_A C_{B\max} = 3.4 \times 10^{-5}$; (c) $z = 0.9$ $C_A C_{B\max} = 1.3 \times 10^{-4}$.

averaged conservation equation for the chemical species A (a similar equation holds for species B):

$$\frac{\partial \overline{C_A}}{\partial t} + \frac{\partial}{\partial z}\left(\overline{w}\,\overline{C_A} + \overline{w' C_A'}\right) = -n\mathrm{Da_d}(1 + I_s)\overline{C_A}\,\overline{C_B} + \mathrm{Le}^{-1}\frac{\partial^2 \overline{C_A}}{\partial z^2}, \quad (16)$$

where the overbar signifies a horizontal average and the prime signifies a deviation from this average. In Eq. (16) the intensity of segregation I_s appears (Danckwerts 1952), which is defined as

$$I_s = \frac{\overline{C_A' C_B'}}{\overline{C_A}\,\overline{C_B}}, \quad (17)$$

where $\overline{C_A' C_B'}$ is the horizontally averaged covariance.

Here $I_s = 0$ implies that the covariance is zero and consequently turbulence has mixed the two chemical species perfectly. When the species are completely segregated, the intensity of segregation will have a limiting value $I_s = -1$ and the reaction will be confined to an infinitely thin zone. A positive covariance would mean an increased reaction rate compared to the perfectly mixed case. In the situation studied here where both

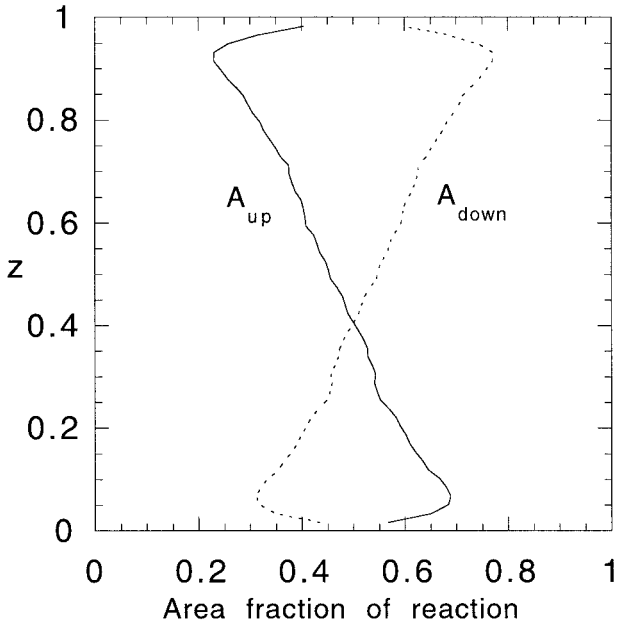

FIG. 5. Vertical profile of the area fraction of chemical reaction ($Da_d = 4.6 \times 10^4$).

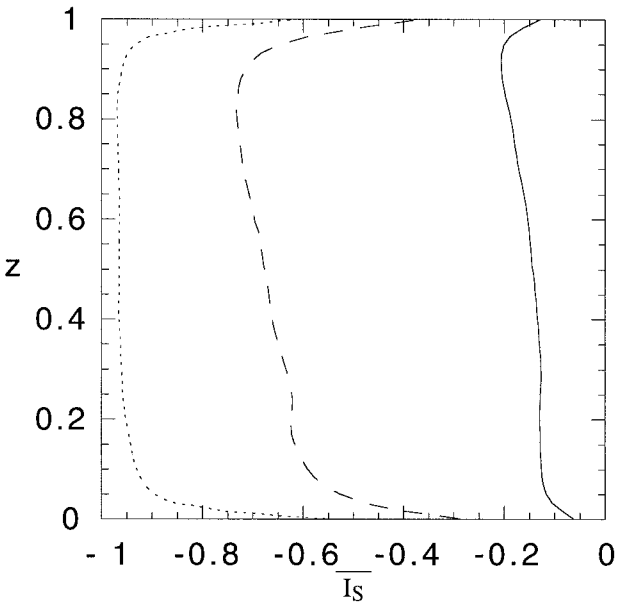

FIG. 6. Vertical profile of the intensity of segregation [Eq. (21)]: solid line, $Da_d = 4.6 \times 10^3$; dashed line, $Da_d = 4.6 \times 10^4$; dotted line, $Da_d = 4.6 \times 10^5$.

species are introduced at opposite boundaries, the intensity of segregation is always negative.

Schumann (1989) was the first to calculate I_s for the CBL, using an LES. In his study, he found that I_s clearly depends on the Damköhler number and the flux ratio n. Only if the fluxes of the two species are equal will the intensity of segregation reach a quasi-steady state. If the fluxes are not equal, I_s will be time dependent since it depends on the actual averaged concentrations of the two chemical species. In spite of this disadvantage (the correlation coefficient could be another variable that indicates the mixing state of chemical species), I_s is still the variable that has to be parameterized since it appears explicitly in the horizontally averaged conservation equations of chemical species (16). Figure 6 shows the intensity of segregation as a function of height for three different Damköhler numbers. All the profiles are similar in shape; smaller (negative) values at the reaction zones near the boundaries and larger (negative) values in the bulk of the CBL indicating an increasing segregation of the species in the bulk. As the segregation becomes more complete with height an extreme value for I_s is found around $z = 0.9$ (with a possible exception for the case with the fastest chemistry $Da_d = 4.6 \times 10^5$ where an extremal value is difficult to define) in agreement with Schumann (1989), who also found the largest (negative) value of I_s near the upper boundary. Although different boundary conditions were applied at the top of the domain, for the case $Da_t = 1$ and $n = -1$, Schumann (1989) obtained a minimum value around $z = 0.9$ (see Fig. 13 in his paper). From Fig. 6 it is clear that for the largest Damköhler number ($Da_t = 13.27$) the intensity of segregation away from the boundaries is close to -1.0, indicating an almost complete segregation of chemical species, which means that chemical reaction is almost absent.

To quantify the limitation of chemical reactions by turbulence, the volume-averaged conservation equation for the chemical species is introduced, which follows in a straightforward way from (2):

$$\frac{\partial \langle C_A \rangle}{\partial t} = -n\mathrm{Da_d}(1 + I_s^{\langle\rangle})\langle C_A\rangle\langle C_B\rangle + \mathrm{Le}^{-1}, \quad (18)$$

where $\langle\ \rangle$ indicates a volume average. The volume intensity of segregation $I_s^{\langle\rangle}$ is defined as

$$I_s^{\langle\rangle} = \frac{\langle C_A' C_B' \rangle}{\langle C_A\rangle\langle C_B\rangle}, \quad (19)$$

where $\langle C_A' C_B' \rangle$ is now the volume-averaged covariance. Note that a prime now indicates a deviation from the volume-averaged quantities. Now an effective reaction rate k_e and an effective Damköhler number can be introduced that quantify the effect of the intensity of segregation:

$$k_e = k(1 + I_s^{\langle\rangle}) \quad (20a)$$

$$\mathrm{Da_e} = \mathrm{Da_t}(1 + I_s^{\langle\rangle}) = \frac{H}{w_c^*} k_e \langle C^* \rangle. \quad (20b)$$

The ratio of Da_e and Da_t indicates the reduction of the reaction rate due to the segregation of the chemical species. The limiting effect of turbulence on chemical reactions is studied by comparing the effective Damköhler

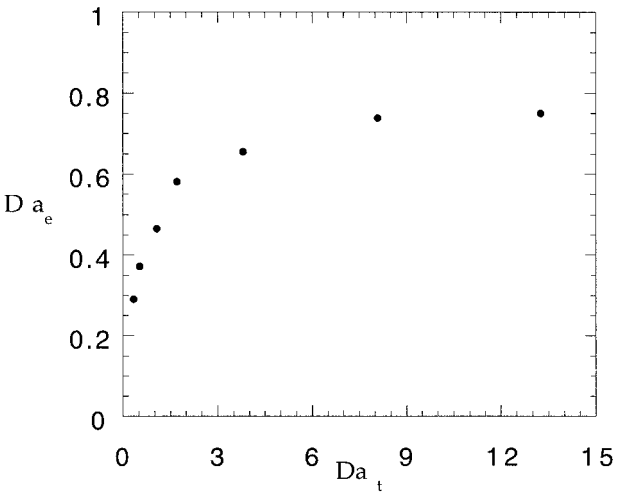

FIG. 7. Turbulent Damköhler number vs effective Damköhler number.

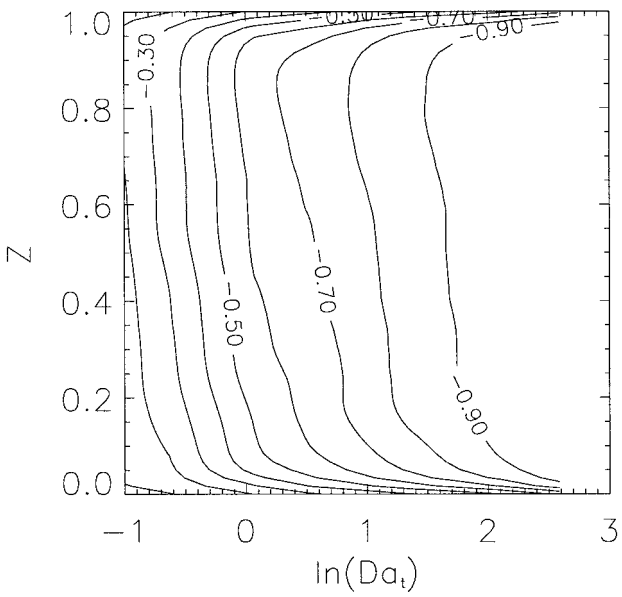

FIG. 8. Intensity of segregation as a function of the turbulent Damköhler number and height.

number to the turbulent Damköhler number (Fig. 7). For values of Da_t larger that 8, Da_e approaches an asymptotic value of around 0.8, signifying a chemical reaction timescale that is of the same order as the integral turbulent timescale. In other words, in situations such as studied here, the chemical reaction timescale has a lower limit that is defined by the timescale of turbulence.

The results shown in Fig. 7 confirm the necessity to parameterize the influence of the segregation of chemical species on chemical reactions under convective conditions in atmospheric chemistry models. Clearly, instead of proceeding at the rate that is given by Da_t, the reaction proceeds at slower timescale that is indicated by Da_e. For instance, at $Da_t = 1$ the ratio $Da_t/Da_e \approx 0.3$, indicating a reaction rate that is only 30% of the expected reaction rate in conditions where the species are perfectly mixed. Figure 8 shows the I_s as a function of the Da_t and z calculated for a flux ratio $n = -1$. Effective chemical reaction rates can be calculated if one has an estimate of the turbulent Damköhler number. For the application to one-dimensional models with a more complex chemistry, lookup tables based on similar figures as Fig. 8 could be be used to obtain an indication of how chemical reaction rates should eventually be corrected. To get an indication of what of atmospheric reaction rates should be corrected due to segregation of the species, we have to consider the integral timescale of turbulence in the atmospheric CBL, which is typically of the order of 15 min. Consequently, chemical reactions as discussed here that have a reaction rate with a similar or smaller timescale should be adjusted accordingly.

More detailed descriptions of the effects of segregation of chemical species in the CBL can be based on models that are similar to the ones developed by Chatfield and Brost (1987) and Randall et al. (1992), where the main features of the CBL are taken into account.

6. Conclusions

A direct numerical simulation is used to study the effect of a convective turbulent flow on chemical reactions in an archetypical situation. In all simulations, the characteristics of the flow are kept constant. Two reactive species are introduced in this convectively driven flow, simulating a bottom-up and top-down diffusion. The chemical species react with an isothermal second-order chemical reaction. The fluxes of the two species are equal and therefore the volume-averaged concentration of the chemical species reaches a quasi-steady state when the sink due to the reaction equals the source at the boundaries.

Various simulations are carried out for a range of chemical reaction rates. To classify the turbulent reacting flow, two Damköhler numbers are defined. The first accounts for the influence of large eddies on the chemical reactions, that is, the turbulent Damköhler number Da_t. The second relates the smallest turbulent scales, characterized by the Kolmogorov timescale to the chemical reaction timescale: the Kolmogorov Damköhler number Da_k. According to this classification, all our simulations are in the regimes of slow and moderate chemistry, where one should expect the largest influence of turbulence on chemical reactions. In all the simulations performed, the Kolmogorov Damköhler number was less than 1; therefore, the smallest chemical scales are always larger than the smallest (Kolmogorov) scales of the flow. As a consequence, all the relevant scales of the turbulent reacting flows are taking into account.

The results show that the reaction zones are located close to the areas where the species are introduced.

Thus, at the bottom of the domain around 70% (maximum value) of the reaction occurs in the core of the updrafts. A slightly higher percentage (maximum value of 80%) is found at the top, but now located in the downdrafts. In the bulk of the CBL the species are almost completely segregated for values of $Da_t = O(1)$ or larger. This effect is quantified by the intensity of segregation (I_s), which depends strongly on the turbulent Damköhler number. The minimum values of I_s are found in the bulk (ranging from -0.15 for the lowest Damköhler number to -0.95 for the highest Damköhler number). In the CBL bulk, chemical reaction is located at the interface between the updraft and the downdraft. However, the amount of reaction at the interface in the bulk is lower than the amount of reaction at the bottom and top of the CBL. The reason is that the horizontal entrainment between up- and downdrafts is much larger at the two boundaries. An adequate representation of the regions near the horizontal boundaries is fundamental to calculate the concentration distribution of species in the CBL.

The way in which the turbulence controls chemical reactions is quantified by introducing an effective Damköhler number. In this dimensionless number, the turbulent characteristics of the CBL are taken into account by introducing the intensity of segregation. The effective Damköhler number has an asymptotic behavior for values of the turbulent Damköhler number larger than 8, with an asymptotic value of about 0.8. In other words, chemical reactions that are categorized as fast when measured under homogeneous laboratory conditions are limited by the turbulent characteristics of the CBL due to incomplete mixing. Consequently, under such conditions, these reactions will proceed at a slower reaction rate. The introduction of the *effective* reaction rate k_e (or Da_e) into global or regional models that simulate atmospheric chemistry and assume species to be perfectly mixed within a grid box will account for these reduced reaction rates by quantifying the effect of the segregation of the chemical species. The Damköhler numbers can also be used to establish a classification of chemical reactions in the atmosphere. The influence of turbulence on chemical reactions can be introduced into more complex atmospheric chemistry models by means of the effective chemical reaction rate or by means of implementing models, which explicitly take the turbulent characteristics of the CBL into account.

Acknowledgments. All computations were performed on the CRAY C98 at the Academic Computing Center (SARA), Amsterdam, the Netherlands. Use of these computing facilities was sponsored by the Stichting Nationale Supercomputer Faciliteiten (National Computing Facilities Foundation, NCF) with financial support from the Nederlandse Organisatie voor Wetenschappelijk Onderzoek (Netherlands Organization for Scientific Research, NWO). We thank Peter Duynkerke for his valuable comments and Sheila McNab for her editing assistance. We also thank Jan Primus for creating an atmosphere that facilitated the discussions.

REFERENCES

Beets, C., M. J. Molemaker, and J. Vilà-Guerau de Arellano, 1996: Direct numerical simulation and large-eddy simulation of a nonpremixed binary reaction in a turbulent convective boundary layer. *Engineering Turbulence Modeling and Measurements*, W. Rodi and G. Bergeles, Eds., Elsevier, Vol. 3, 279–282.

Bilger, R. W., 1980: Turbulent flows with nonpremixed reactants. *Turbulent Reacting Flows*, P. A. Libby and F. A. Willimas, Eds., Springer-Verlag, 243 pp.

Chatfield, R. B., and R. A. Brost, 1987: A two-stream model of the vertical transport of trace species in the convective boundary layer. *J. Geophys. Res.*, **92,** 13 262–13 276.

Colenman, G. N., J. H. Ferziger, and P. R. Spalart, 1990: A numerical model of the turbulent Ekman layer. *J. Fluid Mech.*, **213,** 313–348.

Danckwerts, P. V., 1952: The definition and measurement of some characteristics of mixtures. *Appl. Sci. Res.*, **18A,** 25–60.

Deardorff, J. W., 1972: Numerical investigation of neutral and unstable planetary boundary layer. *J. Atmos. Sci.*, **29,** 91–115.

——, and G. E. Willis, 1967: Investigation of turbulent thermal convection between horizontal plates. *J. Fluid Mech.*, **28,** 675–704.

Dennis, R. L., D. W. Byun, J. H. Novak, K. J. Gallupi, C. J. Coats, and M. A. Vouk, 1996: The next generation of integrated air quality modeling: EPA's models-3. *Atmos. Environ.*, **30,** 1925–1938.

Donaldson, C. du P., and G. R. Hilst, 1972: Effect of inhomogeneous mixing on atmospheric photochemical reactions. *Environ. Sci. Technol.*, **6,** 812–816.

Galperin, B., and S. A. Orszag, 1993: *Large-Eddy Simulation of Complex Engineering and Geophysical Flows.* Cambridge University Press, 600 pp.

Gao, W., and M. L. Wesley, 1994: Numerical modeling of the turbulent fluxes of chemically reactive trace gases in the atmospheric boundary layer. *J. Appl. Meteor.*, **33,** 835–847.

Grotzbach, G., 1982: Direct numerical simulation of laminar and turbulent Benard convection. *J. Fluid Mech.*, **35,** 27–53.

——, 1983: Spatial resolution requirements for direct numerical simulation of the Rayleigh–Benard convection. *Comp. Phys.*, **49,** 241–264.

Herring, J. K., and J. C. Wyngaard, 1987: Convection with a first-order chemically reactive passive scalar. *Turbulent Shear Flows*, Vol. 5, Springer-Verlag, 324–336.

Lenschow, A. A., and A. A. Stephans, 1980: The role of thermals in the convective boundary layer. *Bound.-Layer Meteor.*, **19,** 509–532.

Libby, P. A., and F. A. Willimas, 1980: *Turbulent Reacting Flows.* Springer-Verlag, 243 pp.

Moeng, C.-H., 1984: A large-eddy-simulation model for the study of planetary boundary layer turbulence. *J. Atmos. Sci.*, **41,** 2052–2062.

——, and J. C. Wyngaard, 1984: Statistics of conservative scalars in the convective boundary layer. *J. Atmos. Sci.*, **41,** 3161–3169.

——, and R. Rotunno, 1990: Vertical-velocity skewness in the buoyancy-driven boundary layer. *J. Atmos. Sci.*, **47,** 1149–1162.

Piper, M., J. C. Wyngaard, W. H. Snyder, and R. E. Lawson Jr., 1995: Top-down, bottom-up diffusion experiments in a water convection tank. *J. Atmos. Sci.*, **52,** 3607–3619.

Randall, D. A., Q. Shao, and C. H. Moeng, 1992: A second-order bulk model. *J. Atmos. Sci.*, **49,** 1903–1923.

Riley, J. J., R. W. Metcalfe, and S. A. Orszag, 1986: Direct numerical simulation of chemically reacting turbulent mixing layers. *Phys. Fluids*, **29,** 406–422.

Schumann, U., 1989: Large-eddy simulation of turbulent diffusion

with chemical reactions in the convective boundary layer. *Atmos. Environ.,* **23,** 1713–1727.

——, 1993: Transport asymmetry in skewed convective circulations. *J. Atmos. Sci.,* **50,** 116–119.

Seinfeld, J. H., 1986: *Atmospheric Chemistry and Physics of Air Pollution.* John Wiley and Sons, 738 pp.

Stockwell, W. R., 1995: Effects of turbulence on gas-phase atmospheric chemistry: Calculation of the relationship between time scales for diffusion and chemical reaction. *Meteor. Atmos. Phys.,* **57,** 159–171.

Sykes, R. I., F. Parker, D. S. Henn, and W. S. Llewellen, 1994: Turbulent mixing with chemical reaction in the planetary boundary layer. *J. Appl. Meteor.,* **33,** 825–834.

Tennekes, H., and P. Lumley, 1973: *A First Course in Turbulence.* The MIT Press, 300 pp.

Vilà-Guerau de Arellano, J., P. G. Duynkerke, and K. F. Zeller, 1995: Atmospheric surface layer similarity theory applied to chemically reactive species. *J. Geophys. Res.,* **100,** 1397–1408.

Wyngaard, J. C., and R. A. Brost, 1984: Top-down and bottom-up diffusion of a scalar in the convective boundary layer. *J. Atmos. Sci.,* **41,** 102–112.

——, and J. C. Weil, 1991: Transport asymmetry in skewed turbulence. *Phys. Fluids,* **A3,** 155–162.

——, W. T. Pennell, D. H. Lenschow, and M. A. LeMone, 1978: The temperature-humidity covariance budget in the convective boundary layer. *J. Atmos. Sci.,* **35,** 47–58.